Jarosite

Peter Cogram, University of London, London, United Kingdom

Importance of Jarosite-Family Minerals in the Environment and Hydrometallurgy

Jarosites form a family of iron hydroxysulphate minerals that commonly occur as secondary products in acidic (pH < 3.0) (Brown, 1971; Amoros et al., 1981), sulfate-rich environments formed by the oxidation of sulfide minerals, especially pyrite (FeS_2), and in ore processing wastes (Baron and Palmer, 1996; Welch et al., 2008). The environments that jarosite minerals commonly form in include oxidized zones (gossans) of sulfide deposits (Brown, 1971; Craddock, 1995), areas of acid rock drainage and acid mine drainage (AMD), mine wastes, and acid sulfate soils from pyrite-bearing sediments (Brophy and Sheridan, 1965; Brown, 1971; Baron and Palmer, 1996; Dutrizac and Jambor, 2000; Becker and Gasharova, 2001; Welch et al., 2008; Murphy et al., 2009). Jarosite precipitation is also used for industrial uses and contaminated land remediation (Welch et al., 2007). In hydrometallurgy, especially the zinc industry, the precipitation of jarosite group phases is used in the processing of sulfide ore minerals to control iron (Fe), sulfate (SO_4), alkali metals and other impurities (Dutrizac and Jambor, 1984; Groat et al., 2003; Murphy et al., 2009). These jarosites can contain metals such as cadmium (Cd), copper (Cu), lead (Pb), nickel (Ni), and zinc (Zn), as well as silver (Ag) (Sanchez et al., 1996; Ju et al., 2013; Kerolli-Mustafa et al., 2015). Significant losses of silver can occur in the precipitation of jarosites in hydrometallurgical circuits (Dutrizac and Jambor, 1984), as well as in tailings as a by-product of the processing of economically important minerals (Cabri, 1987).

End-member jarosite sensu stricto contains potassium (K) and has the chemical formula $KFe_3(SO_4)_2(OH)_6$, while other end-member minerals in the jarosite group also contain iron (Fe^{3+}) and sulfur (S^{6+}) (Scott, 1987; Jambor, 1999; Dutrizac and Jambor, 2000). In other end-member jarosite minerals, K^+ is replaced by, for example, sodium (Na^+) in natrojarosite, ammonium (NH_4^+) in ammoniojarosite, hydronium (H_3O^+) in hydronium jarosite, silver (Ag^+) in argentojarosite and lead (Pb^{2+}) in plumbojarosite (Jambor, 1999; Dutrizac and Jambor, 2000). Extensive element substitution may take place in the jarosite crystal structure (Scott, 1990; Jambor, 1999; Dutrizac and Jambor, 2000), which has the ability to incorporate 'much of the Periodic Table' as minor and trace elements (Burger et al., 2009). For example, element substitution in jarosite family minerals may result in Fe^{3+} being replaced by aluminium (Al^{3+}), chromium (Cr^{3+}), copper (Cu^{2+}), gallium (Ga^{3+}) or vanadium (V^{3+}) (Dutrizac and Jambor, 2000; Basciano, 2008; Hudson-Edwards et al., 2008; Murphy et al., 2009) and in S^{6+} being replaced by phosphorus (P^{5+}) or arsenic (As^{5+}) (Jambor, 1999; Dutrizac and Jambor, 2000; Basciano, 2008).

Element substitution means that, in environments such as mine wastes, jarosite minerals are able to scavenge and act as sinks for potentially toxic elements such as As, Cr, Cu and Pb (Smith et al., 2006; Hudson-Edwards et al., 2008; Murphy et al., 2009; Kerolli-Mustafa et al., 2015) and precious metals such as Ag (Ju et al., 2013) that escaped extraction or were mobilized in the natural environment. The take-up of elements by jarosite may also take place at the mineral boundary through sorption or coprecipitation (Smith et al., 2006). In addition, jarosite minerals are potential sources of acid generation (Desborough et al., 2010) and break down readily to release sulfate (SO_4^{2-}) and hydrogen (H^+) ions, as well as metal cations including Fe^{3+}, K^+, trace metals and other contaminants, into stream systems when they are removed from their stability region and dissolve (Smith et al., 2006; Welch et al., 2008). For example, arsenic released by oxidation of As-bearing sulfide minerals, such as pyrite, can be taken up by jarosites formed in mineralized outcrops and mine tailings, and subsequent weathering of the jarosite crusts, which are vulnerable to storm erosion, may be a source for the transport of As into watersheds (Savage et al., 2005).

Argentojarosite and Ag-bearing plumbojarosite can be valuable ores of the precious metal Ag (Dutrizac and Jambor, 1984; Craddock, 1995). The main mineral sources of Ag include jarosites formed in supergene enrichment zones below the upper, oxidized zones (gossans) of orebodies (Hahn, 1929; Craddock, 1995). By contrast to Ag, the precious metal gold (Au) is not known to substitute for K^+ in jarosite (Fairchild, 1933; Jambor, 1999), but Au associated with jarosite in gossans has been reported (Darke et al., 1997).

Chemistry of Jarosite Family Minerals

Jarosite-family minerals form part of the isostructural alunite supergroup, which has the general chemical formula $AB_3(TO_4)_2(OH)_6$ (Jambor, 1999; Dutrizac and Jambor, 2000; Smith et al., 2006). There is extensive element substitution in the *A*, *B*, and *T* sites in the alunite supergroup, which contains >40 end-member natural minerals (Jambor, 1999; Dutrizac and Jambor, 2000; Basciano, 2008). The *A* site of the various end-member alunite-supergroup minerals contains a total of 16 different ions: K, Na, H_3O, Ag, Pb, NH_4, Cu, Tl, Ca, Ba, Sr, Ce, La, Nd, Bi, and Th (Jambor, 1999; Dutrizac and Jambor, 2000; Basciano, 2008). In the alunite supergroup, the *T* site contains S^{6+}, As^{5+}, and/or P^{5+}, as well as Si^{4+} in two end-member minerals (Scott, 1987; Jambor, 1999; Dutrizac and Jambor, 2000). In the supergroup, the *B* site contains Al^{3+} or Fe^{3+}, as well as Ga^{3+} and V^{3+} in one mineral each (Dutrizac and Jambor, 2000; Basciano, 2008). Alunite minerals contain $Al^{3+} > Fe^{3+}$ occupying the *B* site, while in jarosite minerals *B*-site occupation is $Fe^{3+} > Al^{3+}$ (Jambor, 1999; Dutrizac and Jambor, 2000); in natural alunite and jarosite samples, extensive substitution between Al and Fe has been reported (Scott, 1987).

The jarosite family of end-member minerals contains the jarosite group (see Table 1) plus two members of the beudantite group ($Fe^{3+} > Al^{3+}$)—beudantite $PbFe_3[(As,S)O_4]_2(OH,H_2O)_6$ and corkite $PbFe_3[(P,S)O_4]_2(OH,H_2O)_6$—and six members of the crandallite group ($Fe^{3+} > Al^{3+}$)—benauite $SrFe_3(PO_4)_2(OH,H_2O)_6$, kintoreite $PbFe_3(PO_4)_2(OH,H_2O)_6$, lusungite (Sr,Pb) $Fe_3(PO_4)_2(OH,H_2O)_6$, zairite $BiFe_3(PO_4)_2(OH)_6$, dussertite $BaFe_3(AsO_4)_2(OH)_5$, and segnitite $PbFe_3(AsO_4)_2(OH,H_2O)_6$. End-member jarosite group minerals contain S^{6+} in the *T* site, whereas in the beudantite group there is As—S and P—S substitution and in the crandallite group P and As replace S (Jambor, 1999; Dutrizac and Jambor, 2000; Basciano, 2008). The jarosite group comprises eight minerals (see Table 1), including jarosite sensu stricto, natrojarosite, hydronium jarosite, argentojarosite, and plumbojarosite (Dutrizac and Kaiman, 1976; Jambor, 1999; Dutrizac and Jambor, 2000; Drouet and Navrotsky, 2003). Analogues of all these minerals have been synthesized. Mercury jarosite $[Hg_{0.5}Fe_3(SO_4)_2(OH)_6]$ and rubidium jarosite $[RbFe_3(SO_4)_2(OH)_6]$ have also been synthesized but no natural examples are known (Dutrizac and Kaiman, 1976; Jambor, 1999). However, natural and synthetic jarosite minerals rarely have end-member compositions (Welch et al., 2008). Hydronium (H_3O) often substitutes for cations in the *A* site of jarosite (Majzlan et al., 2004; Basciano and Peterson, 2007), and the presence of H_3O as a substitute ion in the *A* site has been demonstrated by the use of nuclear magnetic resonance (NMR) spectroscopy (Ripmeester et al., 1986).

Minerals of the alunite supergroup have the ability to incorporate many minor and trace elements into their crystal structure (Burger et al., 2009). A wide range of combinations of elements is possible in the *A*, *B*, and TO_4 sites. Reported substitutions in the *A* site include Mn^{2+}, Mo^{2+} and ions of end-member alunite supergroup members Na^+, H_3O^+, Pb^{2+}, Ca^{2+}, Sr^{2+}, Ba^{2+}, Nd^{3+}, Ce^{3+}, and La^{3+}, as well as other rare earth elements Sm, Eu, Dy, Er, and Yb; reported substitutions in the *B* site include Pb^{2+}, Mg^{2+}, Zn^{2+}, In^{3+}, Sb^{3+}, Cr^{3+}, and Ti^{4+}, as well as ions of end-member alunite supergroup members Cu^{2+}, V^{3+} and Ga^{3+}; and reported substitutions in the *T* site include Cr^{6+}, Se^{6+}, and Sb^{5+}, as well as P^{5+} and As^{5+} (Scott, 1987; Elgersma et al., 1993; Jambor, 1999; Sejkora et al., 2001; Paktunc and Dutrizac, 2003; Welch et al., 2007, 2008; Burger et al., 2009). In addition, a reported substitution for TO_4^{2-} is CO_3^{2-} (Scott, 1987). Reported substitutions in the OH^- site are Cl^-, F^-, and H_2O (Scott, 1987; Sejkora et al., 2001; Burger et al., 2009).

In synthetic jarosite, reported substitutions for S in the *T* site are As, Se, and Cr, with a maximum As substitution of 17 mol% $AsO_4/(AsO_4 + SO_4)$, or $As/(As + S) = 0.17$ (Paktunc and Dutrizac, 2003). In synthesized jarosite- and alunite-group phases and analogues, substitution between Al^{3+}, Fe^{3+}, Cr^{3+}, and V^{3+} in the *B* site has been reported (Murphy et al., 2009).

There is a strong relationship between occupancy of the crystallographic sites to maintain charge balance in alunite- and jarosite-group minerals (Scott, 1987; Burger et al., 2009). For example, studies have demonstrated coupled substitution of Pb^{2+} (Scott, 1987) and of Ba^{2+} and Sr^{2+} (Burger et al., 2009) for alkali cations in the monovalent *A* site combined with trivalent anions PO_4^{3-} and AsO_4^{3-} for SO_4^{2-} in the *T* site. In addition, a study of alunite supergroup minerals has reported the substitution of AsO_3OH for AsO_4 and of PO_3OH for PO_4 to maintain charge balance where there are substitutions or vacancies in the *A* and *B* sites (Sejkora et al., 2001).

Table 1 End-member minerals of the jarosite group and synthetic analogues

Mineral name	*Formula*	*Synthetic analogue*	*References*
Jarosite	$KFe_3(SO_4)_2(OH)_6$	Potassium jarosite	Jambor (1999), Dutrizac and Jambor (2000), Drouet and Navrotsky (2003), Smith (2004), Basciano (2008), and Hudson-Edwards et al. (2008)
Natrojarosite	$NaFe_3(SO_4)_2(OH)_6$	Sodium jarosite	
Hydronium jarosite	$(H_3O)Fe_3(SO_4)_2(OH)_6$	Hydronium jarosite	
Argentojarosite	$AgFe_3(SO_4)_2(OH)_6$	Silver jarosite	
Plumbojarosite	$Pb_{0.5}Fe_3(SO_4)_2(OH)_6$	Lead jarosite	
Ammoniojarosite	$(NH_4)Fe_3(SO_4)_2(OH)_6$	Ammonium jarosite	
Beaverite	$Pb(Fe,Cu)_3(SO_4)_2(OH)_6$	Lead Fe-Cu-jarosite	
Dorallcharite	$Tl_{0.8}K_{0.2}Fe_3(SO_4)_2(OH)_6$	Thallium jarosite	
No natural mineral	$Hg_{0.5}Fe_3(SO_4)_2(OH)_6$	Mercury jarosite	Dutrizac and Kaiman (1976) and Jambor (1999)
No natural mineral	$RbFe_3(SO_4)_2(OH)_6$	Rubidium jarosite	

In non-stoichiometric jarosite group minerals in which there are deficiencies in occupancy of K^+, Na^+ or other substitute ions in the *A* site, studies often assume the site is occupied by hydronium (H_3O) (Basciano and Peterson, 2007; Desborough et al., 2010); however, occupancy by H_3O is not necessarily the case and often there may be vacancies in the *A* site (Majzlan et al., 2004).

Deficiencies in the *B* site are also reported to be charge balanced by the incorporation of water, in the form of hydronium, into the jarosite structure (Hudson-Edwards et al., 2008). Studies of natural alunite supergroup minerals have reported deficiencies in the *B* site (Scott, 1987; Rattray et al., 1996; Roca et al., 1999) and studies of synthesized jarosite-group minerals have shown deficiencies of Fe in the *B* site (Dutrizac and Kaiman, 1976; Basciano and Peterson, 2007, 2008; Hudson-Edwards et al., 2008). However, a vacancy in the *B* site may be compensated for by the addition of $4H^+$ (protonation) at the *B* site to form four *B*-OH_2 bonds per vacancy, so H_3O in the *A* site is not necessary for charge balance, hence vacancies in the *A* site are commonly seen (Kubisz, 1970; Basciano and Peterson, 2007, 2010). In addition, to maintain charge balance where substitutions or vacancies exist in crystallographic sites of alunite supergroup minerals, including jarosite, many studies have assumed the presence of H_2O in the OH^- site (Hendricks, 1937; Rattray et al., 1996; Sejkora et al., 2001; Drouet et al., 2004; Burger, 2009). These considerations have resulted in a modified general chemical formula being proposed for jarosite compounds: $A_{1-x}(H_3O)_xFe_{3-y}[(OH)_{6-3y}(H_2O)_{3y}(SO_4)_2]$ (Kubisz, 1970).

Many solid solutions are complete among most or all synthetic jarosite species (Dutrizac and Jambor, 2000). Studies have reported solid solution involving K^+, Na^+, and H_3O^+ is extensive in synthetic alunite (Parker, 1962) and jarosite (Brophy et al., 1962; Brophy and Sheridan, 1965; Kubisz, 1970; Jambor, 1999; Basciano and Peterson, 2007, 2008). Hydronium jarosite forms a complete solid-solution series with alkali jarosites. In addition, there is a complete solid solution among synthetic K, Na, and NH_4 jarosites (Brophy and Sheridan, 1965). Substitution involving K^+ and Pb^{2+} has also been shown to be extensive in jarosite (Roca et al., 1999). Lead jarosite forms solid-solution series with monovalent jarosites, but the series are not crystallographically perfect because order-disorder often results in superstructure effects in Pb-rich members, with the *c* axis 34 Å (double axis length of monovalent jarosites) in Pb-jarosite (Dutrizac and Jambor, 1984).

However, studies of natural minerals have reported only limited solid solution between K and Na in low-temperature jarosite and natrojarosite (Burger et al., 2009; Desborough et al., 2010), suggesting the presence of a solvus in the jarosite-natrojarosite system at temperatures below about 140°C (Desborough et al., 2010). In one of these studies, hydronium-bearing jarosite was detected in only one relatively young supergene sample, suggesting H_3O-bearing jarosites are unstable over geological timescales. The extent of solid solution between Na, K, and H_3O affects the stability of natural jarosite and natrojarosite minerals (Desborough et al., 2010).

Synthetic Ag jarosite has been proposed to form an unbroken solid-solution series with K-jarosite in the presence of hydronium (Dutrizac and Jambor, 1984, 2000), as well as with Na-H_3O jarosite (Dutrizac and Jambor, 1984). In addition, in synthetic systems, solid solution between Ag-H_3O and Pb-H_3O in jarosite has been reported; however, despite extensive solid solution between Ag-rich and Pb-rich jarosites, end-member compositions have not been achieved because of partial replacement of the non-ferrous metals by hydronium (Dutrizac and Jambor, 1984).

Crystal Structure of the Jarosite Family of Minerals

The crystal system of jarosite minerals is hexagonal and the crystal structure is in space group *R*-3*m* (Figueiredo and Pereira da Silva, 2011), and has trigonal symmetry (Figueiredo and Pereira da Silva, 2011). The structure has three formula units per unit cell ($Z = 3$), and in jarosite sensu stricto $[KFe_3(SO_4)_2(OH)_6]$ the unit cell contains 3 K, 9 Fe, 6 S, 24 O, and 18 (OH).

The structures of minerals in the alunite supergroup, which includes jarosite family minerals, are layered and based on octahedral-tetrahedral sheets (Jambor, 1999; Hawthorne et al., 2000). These sheets are composed of variably distorted *B*-site cations in octahedral coordination (coordination number [CN] = 6) and *T*-site cation in tetrahedral coordination (CN = 4) (see Fig. 1) (Dutrizac, 1983; Jambor, 1999; Figueiredo and Pereira da Silva, 2011). The $B^{3+}O_6$ octahedra are capped by the TO_4 tetrahedra and make up in-plane corner-sharing $B_3(OH)_6(TO_4)_2^-$ trimers, forming the layers (Hawthorne et al., 2000). The interlayer space is filled by monovalent *A*-site ions, which set the interlayer distance (Grohol and Nocera, 2007).

In jarosite, the *B*-site cation is Fe^{3+} in sixfold (octahedral) coordination with four OH^- and two O^{2-}, while the tetrahedra contain SO_4^{2-} (Brophy et al., 1962; Stoffregen et al., 2000). In alunite minerals, the *B* site is filled by Al^{3+}, which can form a solid solution with Fe^{3+}. In the B site, Fe^{3+} preference over Al^{3+} increases at higher acidity (pH < 3), lower temperature and/or increased Eh of formation (more oxidizing conditions) (Brophy et al., 1962; Burger et al., 2009). Other cations that are known to substitute in the *B* site include Zn^{2+}, Mg^{2+}, and V^{4+} (Burger et al., 2009), Ga^{3+} and Cr^{3+} (Drouet and Navrotsky, 2003) and In^{3+} (Baron and Palmer, 2002).

The octahedra occur at the vertices of a 6^3 plane net, forming six-membered rings with the octahedra linked by corner-sharing four OH^- (Hawthorne et al., 2000). At the junction of three six-membered rings is a three-membered ring, and one set of apical vertices of those three octahedra link to a *T*-site tetrahedron. The resultant sheets are held together by interstitial cations and hydrogen bonds (see Fig. 1).

Fe octahedra corner share (four hydroxyls, OH^-) to form sheets perpendicular to the *c* axis (Basciano and Peterson, 2007; Basciano, 2008), and Fe octahedra also corner-share with SO_4 tetrahedra (two oxygens, O^{2-}), aligned along (001), that is,

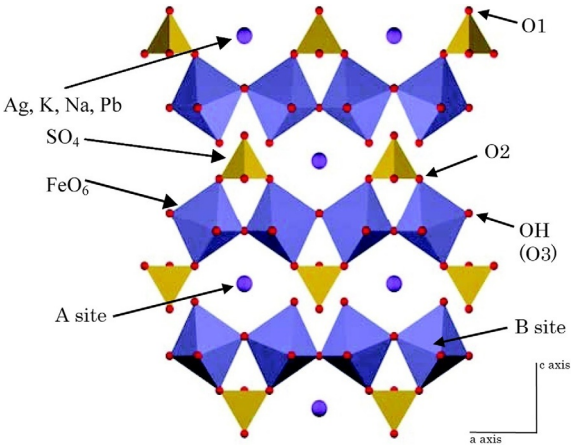

Fig. 1 Jarosite structure of FeO_6 octahedra bonded to (corner-sharing with) SO_4 tetrahedra, forming sheets perpendicular to the *c* axis, with *A*-site ions (e.g., Ag, K, Na, Pb, and H_3O) located between the tetrahedral–octahedral–tetrahedral sheets. Reproduced from Cogram, P. F. (2016). Capacity and mechanisms of uptake of silver by jarosite family minerals. Birkbeck, University of London. PhD thesis published online.

perpendicular to the *c* axis (see Fig. 1) (Jambor, 1999). This means substitutions in the *B* site mainly affect the *a* axis dimension, with *a* decreasing as Al replaces Fe (Jambor, 1999). This is because Fe^{3+} has a larger effective ionic radius (0.645 Å) in sixfold coordination than Al^{3+} (0.535 Å) (Shannon, 1976).

SO_4 tetrahedra, aligned along [001], occur as two crystallographically independent sites within a layer: one set of TO_4 points toward $+c$ ("upward" along the *c* axis), alternating with other set pointing toward $-c$ ("downward" along the *c* axis) (see Fig. 1) (Stoffregen et al., 2000; Basciano and Peterson, 2007; Basciano, 2008). The oxygens and hydroxyls of the octahedra and tetrahedra form an icosahedron, amid which is the *A*-site cation in 12-fold (icosahedral) coordination (CN = 12) (Figueiredo and Pereira da Silva, 2011), with the site filled by monovalent K^+ in end-member jarosite, Na^+ in natrojarosite and Ag^+ in argentojarosite and divalent Pb^{2+} in plumbojarosite. Another monovalent cation that can also fill the *A* site is H_3O^+, which forms the end-member mineral hydronium jarosite.

For compositions with the same TO_4, the length of the *c* parameter of the unit cell is mainly influenced by the size of the *A*-site cation (Jambor, 1999; Stoffregen et al., 2000), with the *c*-axis parameter increasing as the size of the cation increases; the *a*-axis parameter decreases, but to a lesser extent, as cation size increases. For example, in 12-fold coordination, the effective ionic radius of K^+ is 1.64 Å (Å) and Na^+ is 1.39 Å (Shannon, 1976), while for synthesized K-jarosite the *a*-axis is 7.32 Å and the *c*-axis 17.12 Å and for Na-jarosite the *a*-axis is 7.33 Å and the *c*-axis 16.70 Å (Dutrizac and Kaiman, 1976). Such unit-cell variations, which may be revealed by X-ray diffraction data, can be used to estimate the elemental ratios in solid solution between jarosite end-members because the variations are caused by the differences in *A*-site ionic radii (Brophy and Sheridan, 1965; Desborough et al., 2006; Papike et al., 2006).

The Fe^{3+} position in the jarosite structure can be described by a kagome lattice (of interlaced two-dimensional triangles of atoms) (Wills et al., 2004; Basciano and Peterson, 2008). The jarosite group is a main model for studying spin frustration: kagome layers are formed from corner-sharing $Fe^{3+}3$-(μ-OH)$_3$ triangles—the most highly frustrated two-dimensional lattice. Jarosite structures display novel physical properties connected with geometrically frustrated magnetism, such as superconductivity (Grohol and Nocera, 2007).

Occurrence and Importance of Jarosite Family Minerals in the Natural Environment

Environments in which jarosite family minerals commonly form as secondary products include gossans, areas of acid rock drainage and acid mine drainage (AMD), mine tailings, and acidic soils (Dutrizac and Jambor, 2000; Becker and Gasharova, 2001; Welch et al., 2008; Murphy et al., 2009). Jarosites form as secondary (supergene) minerals in the oxidized zones (gossans) of sulphide deposits, particularly at the base of gossans (Craddock, 1995), by the reaction of dilute sulfuric acid (H_2SO_4), Fe^{3+} and other cations such as Ag^+ and Pb^{2+} in ground water with gangue and wall-rock minerals (Brown, 1971; Craddock, 1995). Supergene jarosites are of earthy appearance and have a range of colors, including red (Craddock, 1995).

In the supergene enrichment zones between gossans and sulfide-bearing ore deposits, Ag-bearing jarosite deposits can be an economically important mineral source of silver (Hahn, 1929; Craddock, 1995; Darke et al., 1997; Blowes et al., 2003). An example of supergene Ag-bearing jarosite minerals formed in the oxidation zone of volcanogenic massive sulphide (VMS) deposits is at Rio Tinto, Spain, and such jarosites may also form in the oxidation zones of felsic and mafic volcanic host rocks, as well as other sulphide deposits (Hahn, 1929; Amoros et al., 1981; Craddock, 1995; Roca et al., 1999). Supergene jarosites in oxidized zones can become enriched in Ag compared with the sulphide ore deposits (Darke et al., 1997; Leverett et al., 2005); for example, Rio Tinto

jarosites containing 1000 ppm Ag (0.1%) (Craddock, 1995). In historical times, mines in Rio Tinto and Tharsis, southern Spain, exploited jarosite deposits for Ag (Craddock, 1995), with Ag-bearing jarosite being exploited at Rio Tinto from pre-Roman times (Dutrizac and Jambor, 2000). Argentojarosite was first observed in 1925 as a secondary product from the weathering of sulphide-rich ore veins at Tintic Standard Mine, Dividend, Utah (Dutrizac and Jambor, 2000).

Within saturated (phreatic) or vadose zones of mine tailings and acid sulphate soils, jarosites occur as yellow crusts and coatings (Basciano, 2008). In AMD fluvial environments, jarosite is one of the Fe hydroxides, oxyhydroxides or oxyhydroxysulphates collectively termed "ochre," "boulder coats" or "yellowboy" (Lottermoser, 2003). Ochre commonly occurs as bright reddish-yellow to yellowish-brown stains and coatings, and the precipitates are amorphous, poorly crystalline or crystalline (Lottermoser, 2003).

Jarosite minerals can also form in environments including acidic hypersaline lake sediments and evaporite basins, weathered coal refuse from pyritic coal seams, nodules and disseminations in clays, and hot springs and hydrothermal vents, particularly through gases H_2S and SO_2 being dissolved and oxidized (Brophy and Sheridan, 1965; Dutrizac and Jambor, 2000; Battler et al., 2013). Hypogene jarosite minerals have formed during albitisation, by hydrothermal alteration of alunitised volcanic rocks, as primary argentojarosite in polymetallic ore deposits, and in secondary quartzites (Dutrizac and Jambor, 2000).

Jarosite minerals have been reported in other geological environments that include glauconite sandstones, fillings in cavities in arkoses, bedded cherts, heavy-mineral assemblages in sandstone, and altered quartz porphyry oxidation products (Brophy and Sheridan, 1965). Jarosite, including chromium-jarosite, can form during the corrosion of Portland cement concrete (Becker and Gasharova, 2001; Tazaki et al., 1992). Jarosite-group minerals have accumulated as stalactites and fine-grained mud on massive pyrite in mines (Jamieson et al., 2005). In addition, the presence of jarosite on the surface of Mars has been reported (Papike et al., 2006).

AMD forms from the oxidation of sulphide minerals such as pyrite (FeS_2) and produces acidic waters and secondary minerals such as metal-bearing sulphates, hydrosulphates, such as jarosite, and hydrous oxides, for example goethite (α-FeOOH). Jarosite group minerals form in strong acidity and moderate to highly oxidized sulphate-rich waters. Jarosites occur as yellow crusts and coatings within saturated (phreatic) or vadose zones of mine tailings and acid sulphate soils (Basciano, 2008). Jarosite can form by precipitation of K^+ with Fe^{3+} and $SO_4{}^{2-}$ generated by pyrite oxidation as follows (Blowes et al., 2003; Basciano, 2008):

$$K^+_{(aq)} + 3Fe^{3+}_{(aq)} + 2SO_4{}^{2-} + 6H_2O_{(l)} \leftrightarrow KFe_3(SO_4)_2(OH)_{6(s)} + 6H^+_{(aq)}$$

The equivalent equation applies for the formation of sodium-jarosite (natrojarosite) from Na^+ ions (Casas et al., 2007).

The Fe^{3+} and $SO_4{}^{2-}$ required for jarosite formation can be supplied by processes other than sulphide mineral oxidation. Hypogene jarosites, for example, form as a result of the oxidation of H_2S gas to SO_4 and host-rock Fe^{2+} to Fe^{3+} upon ascent of hydrothermal fluids, and precipitation of the resultant oxidized species. In evaporative environments, the necessary ions for jarosite formation are provided by oxidation of sulphides, Fe(II)-bearing silicates and sulphate aerosols, and acidity from ferrolysis or sulphide oxidation.

Bacteria can metabolize metals and sulfur, accelerating sulphide oxidization, the release of metals into solution and the creation of AMD (Blowes et al., 2003). Bacterial oxidation of Fe^{2+} from pyrite and other sulphides aids the formation of jarosite (Sasaki and Konno, 2000; Becker and Gasharova, 2001). Acid tolerant (acidophile) bacterium *Thiobacillus ferrooxidans* is one of 18 bacteria species and four archaea species that are known oxidisers of pyrite. The process takes place either by direct interaction, with the microbe attaching to the mineral surface and solubilizing it by enzymatic reactions, or by indirect interaction, with reactions taking place close to the mineral surface but not on it (Blowes et al., 2003).

Jarosites in Hydrometallurgy

The precipitation of jarosite group phases is used in hydrometallurgy, especially the zinc industry, to control Fe, sulphate, alkalis and other impurities (Groat et al., 2003; Murphy et al., 2009). Hydrometallurgical treatment of Zn sulphide ore involves separation of Zn from Fe, as most Zn processing concentrates contain 5%–12% Fe. Processes involving the formation of jarosite remove Fe from acidic zinc sulphate solutions prior to Zn electrolysis (Dutrizac and Kaiman, 1976; Arslan and Arslan, 2003).

As well as Fe, these jarosites can contain Ag and other metals such as Cd, Cu, Ni, Pb, Zn (Sanchez et al., 1996; Ju et al., 2013; Kerolli-Mustafa et al., 2015). Argentojarosite and Ag-bearing plumbojarosite can be valuable ores of Ag and Pb, and precipitation of jarosites as controls of Fe and other impurities, including trace metals, in hydrometallurgical circuits can lead to significant losses of Ag (Dutrizac and Jambor, 1984). In hydrometallurgy, much of the Ag present may enter the jarosite fraction and could be a cause of erratic recoveries of Ag "values" (Dutrizac and Kaiman, 1976; Dutrizac and Jambor, 2000), as during conventional cyanidation processing of gossan, precipitation of Ag as silver jarosite can prevent its recovery (Dutrizac and Kaiman, 1976; May et al., 1973); cyanidation under conventional conditions recovers 40% of Ag from gossan ores of Rio Tinto, Spain (Roca et al., 1999).

Synthesis Methods for Jarosite Compounds

The factors affecting the extent of jarosite precipitation and the composition of jarosites are important for mineralogists in terms of understanding the partitioning of alkali ions during jarosite formation in supergene deposits and the extent of element and

hydronium substitution for alkalis (Dutrizac, 1983). Synthetic jarosites are often used in studies as analogues for natural jarosites (Brown, 1970; Desborough et al., 2006; Swayze et al., 2008). Other experiments of jarosite synthesis have been carried out as research on jarosite processes used in the hydrometallurgical industry (Dutrizac and Jambor, 2000). Metallurgists are concerned with the effect of synthesis factors such as temperature, seeding and pH on the yield and composition of the jarosite product (Dutrizac, 1983).

Synthesis experiments to form jarosite minerals have been carried out at least since the 1930s (Fairchild, 1933). A variety of methods have been used in these jarosite syntheses, creating different amounts of product of various chemical compositions. Dutrizac and Jambor (2000) provide a summary of the literature on many of the synthesis parameters of jarosite formation, especially K- and Na-jarosite, and since that time there have been numerous other experiments; for example, Basciano and Peterson (2007 and 2008).

In synthesis experiments on jarosite, most studies have assumed the necessary presence of ferric iron for jarosite formation by using reactant $Fe_2(SO_4)_3$ or $Fe_2(SO_4)_3{\cdot}5H_2O$ to supply Fe(III) to synthesis experiments (Fairchild, 1933; Baron and Palmer, 1996). The lower limit of molar concentration (M, mol dm^{-3}) of Fe(III) for jarosite precipitation is near 10^{-3} M (0.001 M) (Brown, 1971), while synthetic jarosites readily precipitate from sulphate-rich solutions containing 0.025–3.0 M Fe(III) (Brophy et al., 1962; Brophy and Sheridan, 1965; Brown, 1970). To synthesize K-, Na- and Ag-jarosite at 25°C, Brown (1970) used the 1:3 M ratio of (K^+-Ag^+):Fe^{3+} or (Na^+-Ag^+):Fe^{3+} in stoichiometric jarosite. This achieved K^+ occupancy of 97%–100% in synthesized jarosite. In other studies 20% extra ferric sulphate was used (Fairchild, 1933; Brophy et al., 1962), raising the molar ratio to 1:3.6.

Jarosite minerals can be precipitated from solutions with 0.05 M Na^+ (Dutrizac and Jambor, 2000) or 0.02 M K^+ (Brown, 1970). However, very high alkali-sulphate concentrations ($>$ 1.0 M Na_2SO_4) can result in the precipitation of alkali-Fe^{3+} sulphates instead of jarosites (Dutrizac and Jambor, 2000). Slightly excess alkali concentration (i.e., higher than the M^+:Fe^{3+} stoichiometric ratio of 1:3) in the starting solution improves jarosite precipitate yield and alkali content (relative to hydronium content) (Dutrizac and Jambor, 2000). In studies, a wide variety of alkali (K or Na) and substitute ion molar concentrations have been used in the starting solutions in jarosite syntheses; for example, between 0.02 M K^+ and 0.2 M K^+ (K^+:Fe^{3+} 1:3) by Brown (1970), and 0.6 M Na^+ and 0.00048 M Ag^+ (Na^+:Ag^+:Fe^{3+} 1.5:0.0012:1) by Patino et al. (1998).

An equation for the precipitation of jarosites from homogeneous solutions containing alkali (A^+) ions is (Grohol and Nocera, 2007):

$$3Fe^{3+} + 2A_2SO_4 + 6H_2O \rightarrow AFe_3(SO_4)_2(OH)_6 + 3A^+ + 6H^+$$

At least four different types of reactant have been used to supply K, Na and other cations in jarosite synthesis experiments: sulphates (e.g., K_2SO_4 and Na_2SO_4) (Brophy et al., 1962; Brown, 1970; May et al., 1973; Dutrizac and Jambor, 1984); hydroxides (e.g., KOH and NaOH) (Kubisz, 1970); nitrates (e.g., KNO_3 and $NaNO_3$) (Dutrizac and Kaiman, 1976; Frost et al., 2005); and chlorides (e.g., KCl and NaCl) (Basciano and Peterson, 2007 and 2008). Hydroxides, nitrates and chlorides were used instead of sulphates to reduce the sulphate-to-iron ratio in the synthesis solution and so create products with less hydronium content.

Laboratory syntheses of jarosites have been carried out at temperatures ranging from 20°C to 150°C, to simulate natural and engineered (hydrometallurgical) environments, with elevated temperatures helping to speed up the reaction and form purer compounds (Brown, 1970; Dutrizac, 1983; Dutrizac and Jambor, 2000).

The acidity (pH) of the synthesis solution plays a major role in jarosite stability and the amount of precipitate, but has little effect on composition (Dutrizac, 1983; Dutrizac and Jambor, 2000). Dutrizac and Jambor (1984) state that pH values of 1.0–1.6 are near-optimum jarosite synthesis conditions.

Morphology and Grain Size of Synthetic Jarosite Compounds

Scanning electron microscopy (SEM) has been used to produce secondary-electron images of synthetic samples of jarosite group minerals (Gasharova et al., 2005; Cogram, 2016). Crystals of K-H_3O-jarosite generally comprise rounded hexagonal plates on {0001} (Anthony et al., 2003). Crystals of Na-H_3O-jarosite comprise pyramidal {01-12} and {0001} faces and rhombohedral {01-12} faces (Cogram, 2016). Crystals of Ag-H_3O-jarosite comprise intergrown hexagonal plates on {0001} and dipyramidal (octahedral) rhombs with {01-12} and {0001} faces (Gasharova et al., 2005), both sometimes rounded (Cogram, 2016). The crystals are in compact texture and often intergrown and grain sizes are approximately 1–25 μm (see Figs. 2–4).

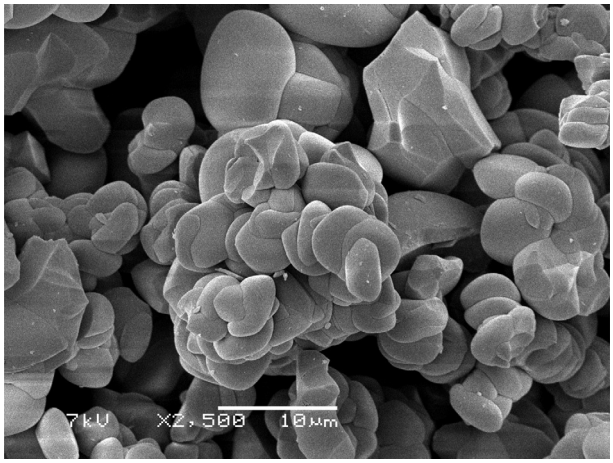

Fig. 2 K-H_3O-jarosite. Reproduced from Cogram, P. F. (2016). Capacity and mechanisms of uptake of silver by jarosite family minerals. Birkbeck, University of London. PhD thesis published online.

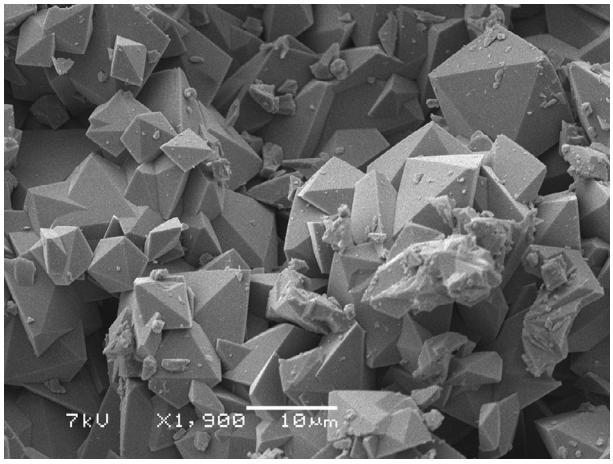

Fig. 3 Na-H_3O-jarosite. Reproduced from Cogram, P. F. (2016). Capacity and mechanisms of uptake of silver by jarosite family minerals. Birkbeck, University of London. PhD thesis published online.

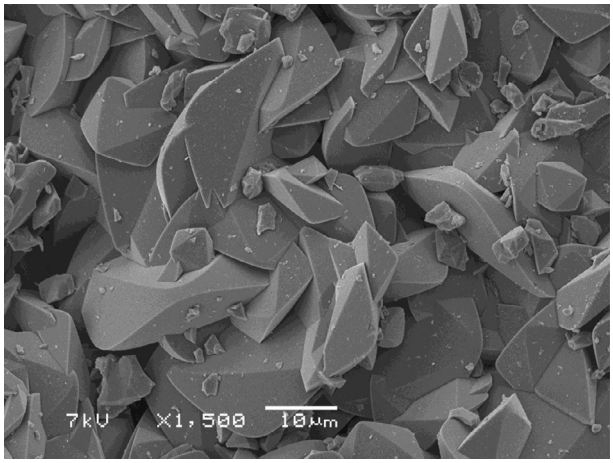

Fig. 4 Ag-H_3O-jarosite. Reproduced from Cogram, P. F. (2016). Capacity and mechanisms of uptake of silver by jarosite family minerals. Birkbeck, University of London. PhD thesis published online.

References

Amoros JL, Lunar R, and Tavira P (1981) Jarosite: A silver-bearing mineral of the gossan of Rio Tinto (Huelva) and La Union (Cartagena, Spain). *Mineralium Deposita* 16: 205–213.

Anthony JW, Bideaux RA, Bladh KW, and Nichols MC (2003) *Handbook of mineralogy*. Chantilly, VA: Mineralogical Society of America. www.handbookofmineralogy.org.

Arslan C and Arslan F (2003) Thermochemical review of jarosite and goethite stability regions at 25 and 95°C. *Turkish Journal of Engineering and Environmental Science* 27: 45–52.

Baron D and Palmer CD (1996) Solubility of jarosite at 4–35°C. *Geochimica et Cosmochimica Acta* 60(2): 185–195.

Baron D and Palmer CD (2002) Solid-solution aqueous-solution reactions between jarosite ($KFe_3(SO_4)_2(OH)_6$) and it chromate analog. *Geochimica et Cosmochimica Acta* 66(16): 2841–2853.

Basciano, L. C., 2008. Crystal chemistry of the jarosite group of minerals: Solid solution and atomic structures. PhD thesis, Queen's University, Kingston, Ontario, Canada, published online.

Basciano LC and Peterson RC (2007) Jarosite-hydronium jarosite solid-solution series with full iron site occupancy: Mineralogy and crystal chemistry. *American Mineralogist* 92: 1464–1473.

Basciano LC and Peterson RC (2008) Crystal chemistry of the natrojarosite-jarosite and natrojarosite-hydronium jarosite solid-solution series: A synthetic study with full iron site occupancy. *American Mineralogist* 93: 853–862.

Basciano LC and Peterson RC (2010) A crystallographic study of the incomplete solid-solution between plumbojarosite and jarosite. *Canadian Mineralogist* 48: 651–659.

Battler MM, Osinski GR, Lim DSS, Davila AF, Michel FA, Craig MA, Izawa MRM, Leoni L, Slater GF, Fairén AG, Preston LJ, and Banerjee NR (2013) Characterization of the acidic cold seep emplaced jarositic golden deposit, NWT, Canada, as an analogue for jarosite deposition on Mars. *Icarus* 224: 382–398.

Becker U and Gasharova B (2001) AFM observations and simulations of jarosite growth at the molecular scale: Probing the basis for the incorporation of foreign ions into jarosite as a storage mineral. *Physics and Chemistry of Minerals* 28: 545–556.

Blowes DW, Ptacek CJ, Jambor JL, and Weisener CG (2003) The geochemistry of acid mine drainage. *Treatise on Geochemistry* 9: 149–204.

Brophy GP and Sheridan MF (1965) Sulphate studies IV: The jarosite-natrojarosite-hydronium jarosite solid solution series. *American Mineralogist* 50: 1595–1607.

Brophy GP, Scott ES, and Snellgrove RA (1962) Sulphate studies II: Solid solution between alunite and jarosite. *American Mineralogist* 47: 112–126.

Brown JB (1970) A chemical study of some synthetic potassium-hydronium jarosites. *Canadian Mineralogist* 10: 696–703.

Brown JB (1971) Jarosite-goethite stabilities at 25C, 1 atm. *Mineralium Deposita* 6: 245–252.

Burger PV, Papike JJ, Shearer JM, and Karner JM (2009) Jarosite growth zoning as a recorder of fluid evolution. *Geochimica et Cosmochimica Acta* 73: 3248–3259.

Cabri LJ (1987) The mineralogy of precious metals: New developments and metallurgical implications. *Canadian Mineralogist* 25: 1–7.

Casas JM, Paipa C, Godoy I, and Vargas T (2007) Solubility of sodium-jarosite and solution speciation in the system Fe(III)–Na–H_2SO_4–H_2O at 70°C. *Journal of Geochemical Exploration* 92: 111–119.

Cogram, P. F., 2016. Capacity and mechanisms of uptake of silver by jarosite family minerals. Birkbeck, University of London. PhD thesis published online.

Craddock PT (1995) *Early metal mining and production*. Washington, DC: Smithsonian Institution press.

Darke KE, Boyce AJ, Clapperton CM, Fallick AE, Redwood SD, and Rice CM (1997) Supergene mineralization at the Koro Kollo gold mine, Bolivia. *Exploration and Mining Geology* 6(3): 209–221.

Desborough GA, Smith KS, Lowers HA, Swayze GA, Hammarstrom JM, Diehl SF, Driscoll RL, and Leinz RW (2006) In: *The use of synthetic jarosite as an analog for natural jarosite, Proceedings of the Seventh International Conference on Acid Rock Drainage (ICARD 7), St Louis, Missouri, USA, March 26–30, 2006,* pp. 458–475.

Desborough GA, Smith KS, Lowers HA, Swayze GA, Hammarstrom JM, Diehl SF, Leinz RW, and Driscoll RL (2010) Mineralogical and chemical characteristics of some natural jarosites. *Geochimica et Cosmochimica Acta* 74: 1041–1056.

Drouet C and Navrotsky A (2003) Synthesis, characterization, and thermochemistry of K-Na-H_3O jarosites. *Geochimica et Cosmochimica Acta* 67(11): 2063–2076.

Drouet C, Pass KL, Baron D, Draucker S, and Navrotsky A (2004) Thermochemistry of jarosite-alunite and natrojarosite-natroalunite solid solutions. *Geochimica et Cosmochimica Acta* 68(10): 2197–2205.

Dutrizac JE (1983) Factors affecting alkali jarosite precipitation. *Metallurgical and Materials Transactions B* 14(4): 531–539.

Dutrizac JE and Jambor JL (1984) In: Park WC, Hausen DM, and Hagni RD (eds.) *Formation and characterization of argentojarosite and plumbojarosite and their relevance to metallurgical processing*, Applied mineralogy 1984: Proceedings of the second international congress on applied mineralogy in the minerals industry, Los Angeles, California, February 22–25, 1984, Warrendale, Pennsylvania: The Metallurgical Society of AIME (the American Institute of Mining, Metallurgical and Petroleum Engineers, Inc.).

Dutrizac JE and Jambor JL (2000) Jarosites and their application in hydrometallurgy. In: Alpers CN, Jambor JL, and Nordstrom DK (eds.) *Sulphate minerals: Crystallography, geochemistry and environmental significance. Reviews in mineralogy and geochemistry*, vol. 40. Washington D.C: Mineralogical Society of America Geochemical Society.

Dutrizac JE and Kaiman S (1976) Synthesis and properties of jarosite-type compounds. *Canadian Mineralogist* 14: 151–158.

Elgersma F, Witkamp GJ, and van Rosmalen GM (1993) Incorporation of zinc in continuous jarosite precipitation. *Hydrometallurgy* 33: 313–339.

Fairchild JG (1933) Artificial jarosites—The separation of potassium from cesium. *American Mineralogist* 18: 543–547.

Figueiredo M-O and Pereira da Silva T (2011) The positive environmental contribution of jarosite by retaining lead in acid mine drainage areas. *International Journal of Environmental Research and Public Health* 8: 1575–1582.

Frost RL, Wills R-A, Weier ML, and Martens W (2005) Thermal decomposition of synthetic argentojarosite—Implications for silver production in medieval times. *Thermochimica Acta* 437: 30–33.

Gasharova B, Gottlicher J, and Becker U (2005) Dissolution at the surface of jarosite: An in-situ AFM study. *Chemical Geology* 215: 499–516.

Groat LA, Jambor JL, and Pemberton BC (2003) The crystal structure of argentojarosite, $AgFe_3(SO_4)_2(OH)_6$. *Canadian Mineralogist* 41: 921–928.

Grohol D and Nocera DG (2007) Magnetic disorder in the frustrated antiferromagnet jarosite arising from the $H_3O^{+}\cdots OH^{-}$ interaction. *Chemistry of Materials* 19: 3061–3066.

Hahn, A. W., 1929. Silver-bearing minerals of some ores from the Tintic mining district. Transactions of AIME, 77, 325–329. Published online at www.aimehq.org/search/docs/Volume%20085/085-42.pdf.

Hawthorne FC, Krivovichev SV, and Burns PC (2000) Crystal chemistry of sulphate minerals. In: Alpers CN, Jambor JL, and Nordstrom DK (eds.) *Sulphate minerals: Crystallography, geochemistry and environmental significance. Reviews in mineralogy and geochemistry.* Vol. 40, pp. 405–452. Washington D.C.: Mineralogical Society of America Geochemical Society.

Hendricks SB (1937) The crystal structure of alunite and the jarosites. *American Mineralogist* 22: 773–784.

Hudson-Edwards KA, Smith AML, Dubbin WE, Bennett AJ, Murphy PJ, and Wright K (2008) Comparison of the structures of natural and synthetic Pb-Cu-jarosite-type compounds. *European Journal of Mineralogy* 20: 241–252.

Jambor JL (1999) Nomenclature of the alunite supergroup. *Canadian Mineralogist* 37: 1323–1341.

Jamieson HE, Robinson C, Alpers CN, Nordstrom DK, Poustovetov A, and Lowers HA (2005) The composition of coexisting jarosite-group minerals and water from the Richmond mine, Iron Mountain, California. *The Canadian Mineralogist* 43: 1225–1242.

Ju S, Zhang L, Peng J, Shi Z, Guo S, Liu B, and Wang Y (2013) Thermodynamics of leaching roasted jarosite residue from zinc hydrometallurgy in NH_4Cl system. *Transactions of Nonferrous Metals Society of China* 23: 1179–1183.

Kerolli-Mustafa M, Fajkovic H, Roncevic S, and Curkovic L (2015) Assessment of metal risks from different depths of jarosite tailing waste of Trepca zinc industry, Kosovo based on BCR procedure. *Journal of Geochemical Exploration* 148: 161–168.

Kubisz J (1970) Studies on synthetic alkali-hydronium jarosites: I. Synthesis of jarosite and natrojarosite. *Mineralogia Polonica* 1: 47–59.

Leverett, P., McKinnon, A. R. and Williams P. A., 2005. Supergene geochemistry of the Endeavor ore body, Cobar, NSW, and relationships to other deposits in the Cobar basin. In: Roach, I. C. (ed.), Regolith 2005—Ten years of CRC LEME: Proceedings of CRC LEME regional regolith Symposia 2005. The Cooperative Research Centre for Landscape Environments and Mineral Exploration, Australia, published online.

Lottermoser BG (2003) *Mine wastes: Characterization, treatment and environmental impacts*. Berlin Heidelberg: Springer-Verlag.

Majzlan J, Stevens R, Boerio-Goates J, Woodfield BF, Navrotsky A, Burns PC, Crawford MK, and Amos TG (2004) Thermodynamic properties, low-temperature heat-capacity anomalies, and single-crystal X-ray refinement of hydronium jarosite, $(H_3O)Fe_3(SO_4)_2(OH)_6$. *Physics and Chemistry of Minerals* 31: 518–531.

May A, Sjoberg JJ, and Baglin EG (1973) Synthetic argentojarosite: Physical properties and thermal behaviour. *American Mineralogist* 58: 936–941.

Murphy PJ, Smith AML, Hudson-Edwards KA, Dubbin WE, and Wright K (2009) Raman and IR spectroscopic studies of alunite-supergroup compounds containing Al, Cr^{3+}, Fe^{3+} and V^{3+} at the *B* site. *The Canadian Mineralogist* 47: 663–681.

Paktunc D and Dutrizac JE (2003) Characterisation of arsenate-for-sulfate substitution in synthetic jarosite using X-ray diffraction and X-ray absorption spectroscopy. *The Canadian Mineralogist* 41: 905–919.

Papike JJ, Karner JM, and Shearer CK (2006) Implications of Martian and terrestrial jarosite: A crystal chemical perspective. *Geochimica et Cosmochimica Acta* 70: 1309–1321.

Parker RL (1962) Isomorphous substitution in natural and synthetic alunite. *American Mineralogist* 47: 127–136.

Patino F, Salinas E, Cruells M, and Roca A (1998) Alkaline decomposition-cyanidation kinetics of argentian natrojarosite. *Hydrometallurgy* 49: 323–336.

Rattray KJ, Taylor MR, Bevan DJM, and Pring A (1996) Compositional segregation and solid solution in the lead-dominant alunite-type minerals from Broken Hills, N.S.W. *Mineralogical Magazine* 60: 779–785.

Ripmeester JA, Ratcliffe CI, Dutrizac JE, and Jambor JL (1986) Hydronium ion in the alunite-jarosite group. *Canadian Mineralogist* 24: 435–437.

Roca A, Vinals J, Arranz M, and Calero J (1999) Characterization and alkaline decomposition/cyanidation of beudantite-jarosite materials from Rio Tinto gossan ores. *Canadian Metallurgical Quarterly* 38(2): 93–103.

Sanchez L, Cruells M, and Roca A (1996) Sulphidization-cyanidation of jarosite species: Applicability to the gossan ores of Rio Tinto. *Hydrometallurgy* 42: 35–49.

Sasaki K and Konno H (2000) Morphology of jarosite-group compounds precipitated from biologically and chemically oxidized Fe ions. *Canadian Mineralogist* 38: 45–56.

Savage KS, Bird DK, and O'Day PA (2005) Arsenic speciation in synthetic jarosite. *Chemical Geology* 215: 473–498.

Scott KM (1987) Solid solution in, and classification of, gossan-derived members of the alunite-jarosite family, Northwest Queensland, Australia. *American Mineralogist* 72: 178–187.

Scott KM (1990) Origin of alunite- and jarosite-group minerals in the Mt. Leyshon epithermal gold deposit, Northeast Queensland, Australia. *American Mineralogist* 75: 1176–1181.

Sejkora J, Cejka J, and Srein V (2001) Lead-dominant members of the crandallite group from Cinovec and Moldava deposits, Krusne hory Mts, Czech Republic. *Journal of the Czech Geological Society* 46(1–2): 53–68.

Shannon RD (1976) Revised effective radii and systematic studies of interatomic distances in halides and chalcogenides. *Acta Crystallographica* A32: 751–767.

Smith, A. M. L., 2004. Mechanisms and products of the breakdown of contaminant element-bearing jarosites. Unpublished PhD thesis, Birkbeck College, University of London.

Smith AML, Hudson-Edwards KA, Dubbin WE, and Wright K (2006) Dissolution of jarosite $[KFe_3(SO_4)_2(OH)_6]$ at pH 2 and 8: Insights from batch experiments and computational modeling. *Geochimica et Cosmochimica Acta* 70: 608–621.

Stoffregen RE, Alpers CN, and Jambor JL (2000) Alunite-jarosite crystallography, thermodynamics and geochronology. In: Alpers CN, Jambor JL, and Nordstrom DK (eds.) *Sulphate minerals: Crystallography, geochemistry and environmental significance, reviews in mineralogy and geochemistry*. Vol. 40. Washington D.C: Mineralogical Society of America/ Geochemical Society.

Swayze GA, Desborough GA, Smith KS, Lowers HA, Hammarstrom JM, Diehl SF, Leinz RW, and Driscoll RL (2008) Understanding jarosite—From mine waste to Mars. In: Verplanck PL (ed.) *Understanding contaminants associated with mineral deposits: USGS circular 1328*, pp. 8–13. Reston, Virginia: US Geological Survey.

Tazaki K, Mori T, and Nonaka T (1992) Microbial jarosite and gypsum from corrosion of Portland cement concrete. *Canadian Mineralogist* 30: 431–444.

Welch SA, Christy AG, Kirste D, Beavis SG, and Beavis F (2007) Jarosite dissolution I—Trace cation flux in acid sulfate soils. *Chemical Geology* 245: 183–197.

Welch SA, Kirste D, Christy AG, Beavis FR, and Beavis SG (2008) Jarosite dissolution II—Reaction, kinetics, stoichiometry and acid flux. *Chemical Geology* 254: 73–86.

Wills AS, Smith AML, Dubbin WE, Hudson-Edwards KA, and Wright K (2004) Interlayer exchange in the plumbo-jarosites: kagomé systems. *Journal of Magnetism and Magnetic Materials* 272–276: 1300–1301.